

University of Nebraska - Lincoln

DigitalCommons@University of Nebraska - Lincoln

Kenneth Bloom Publications

Research Papers in Physics and Astronomy

10-16-2000

Direct Measurement of the W Boson Width in $p\bar{p}$ Collisions at $\sqrt{s} = 1.8$ TeV

T. Affolder

Ernest Orlando Lawrence Berkeley National Laboratory, Berkeley, California

Kenneth A. Bloom

University of Nebraska-Lincoln, kenbloom@unl.edu

Collider Detector at Fermilab Collaboration

Follow this and additional works at: <https://digitalcommons.unl.edu/physicsbloom>



Part of the [Physics Commons](#)

Affolder, T.; Bloom, Kenneth A.; and Fermilab Collaboration, Collider Detector at, "Direct Measurement of the W Boson Width in $p\bar{p}$ Collisions at $\sqrt{s} = 1.8$ TeV" (2000). *Kenneth Bloom Publications*. 99. <https://digitalcommons.unl.edu/physicsbloom/99>

This Article is brought to you for free and open access by the Research Papers in Physics and Astronomy at DigitalCommons@University of Nebraska - Lincoln. It has been accepted for inclusion in Kenneth Bloom Publications by an authorized administrator of DigitalCommons@University of Nebraska - Lincoln.

Direct Measurement of the W Boson Width in $p\bar{p}$ Collisions at $\sqrt{s} = 1.8$ TeV

T. Affolder,²¹ H. Akimoto,⁴³ A. Akopian,³⁶ M. G. Albrow,¹⁰ P. Amaral,⁷ S. R. Amendolia,³² D. Amidei,²⁴ K. Anikeev,²² J. Antos,¹ G. Apollinari,¹⁰ T. Arisawa,⁴³ T. Asakawa,⁴¹ W. Ashmanskas,⁷ M. Atac,¹⁰ F. Azfar,²⁹ P. Azzi-Bacchetta,³⁰ N. Bacchetta,³⁰ M. W. Bailey,²⁶ S. Bailey,¹⁴ P. de Barbaro,³⁵ A. Barbaro-Galtieri,²¹ V. E. Barnes,³⁴ B. A. Barnett,¹⁷ M. Barone,¹² G. Bauer,²² F. Bedeschi,³² S. Belforte,⁴⁰ G. Bellettini,³² J. Bellinger,⁴⁴ D. Benjamin,⁹ J. Bensinger,⁴ A. Beretvas,¹⁰ J. P. Berge,¹⁰ J. Berryhill,⁷ B. Bevensee,³¹ A. Bhatti,³⁶ M. Binkley,¹⁰ D. Bisello,³⁰ R. E. Blair,² C. Blocker,⁴ K. Bloom,²⁴ B. Blumenfeld,¹⁷ S. R. Blusk,³⁵ A. Bocci,³² A. Bodek,³⁵ W. Bokhari,³¹ G. Bolla,³⁴ Y. Bonushkin,⁵ D. Bortoletto,³⁴ J. Boudreau,³³ A. Brandl,²⁶ S. van den Brink,¹⁷ C. Bromberg,²⁵ M. Brozovic,⁹ N. Bruner,²⁶ E. Buckley-Geer,¹⁰ J. Budagov,⁸ H. S. Budd,³⁵ K. Burkett,¹⁴ G. Busetto,³⁰ A. Byon-Wagner,¹⁰ K. L. Byrum,² P. Calafiura,²¹ M. Campbell,²⁴ W. Carithers,²¹ J. Carlson,²⁴ D. Carlsmith,⁴⁴ J. Cassada,³⁵ A. Castro,³⁰ D. Cauz,⁴⁰ A. Cerri,³² A. W. Chan,¹ P. S. Chang,¹ P. T. Chang,¹ J. Chapman,²⁴ C. Chen,³¹ Y. C. Chen,¹ M.-T. Cheng,¹ M. Chertok,³⁸ G. Chiarelli,³² I. Chirikov-Zorin,⁸ G. Chlachidze,⁸ F. Chlebana,¹⁰ L. Christofek,¹⁶ M. L. Chu,¹ C. I. Ciobanu,²⁷ A. G. Clark,¹³ A. Connolly,²¹ J. Conway,³⁷ J. Cooper,¹⁰ M. Cordelli,¹² J. Cranshaw,³⁹ D. Cronin-Hennessy,⁹ R. Cropp,²³ R. Culbertson,⁷ D. Dagenhart,⁴² F. DeJongh,¹⁰ S. Dell'Agnello,¹² M. Dell'Orso,³² R. Demina,¹⁰ L. Demortier,³⁶ M. Deninno,³ P. F. Derwent,¹⁰ T. Devlin,³⁷ J. R. Dittmann,¹⁰ S. Donati,³² J. Done,³⁸ T. Dorigo,¹⁴ N. Eddy,¹⁶ K. Einsweiler,²¹ J. E. Elias,¹⁰ E. Engels, Jr.,³³ W. Erdmann,¹⁰ D. Errede,¹⁶ S. Errede,¹⁶ Q. Fan,³⁵ R. G. Feild,⁴⁵ C. Ferretti,³² R. D. Field,¹¹ I. Fiori,³ B. Flaugher,¹⁰ G. W. Foster,¹⁰ M. Franklin,¹⁴ J. Freeman,¹⁰ J. Friedman,²² H. Frisch,⁷ Y. Fukui,²⁰ S. Galeotti,³² M. Gallinaro,³⁶ T. Gao,³¹ M. Garcia-Sciveres,²¹ A. F. Garfinkel,³⁴ P. Gatti,³⁰ C. Gay,⁴⁵ S. Geer,¹⁰ D. W. Gerdes,²⁴ P. Giannetti,³² P. Giromini,¹² V. Glagolev,⁸ M. Gold,²⁶ J. Goldstein,¹⁰ A. Gordon,¹⁴ A. T. Goshaw,⁹ Y. Gotra,³³ K. Goulianos,³⁶ C. Green,³⁴ L. Groer,³⁷ C. Grosso-Pilcher,⁷ M. Guenther,³⁴ G. Guillian,²⁴ J. Guimaraes da Costa,¹⁴ R. S. Guo,¹ R. M. Haas,¹¹ C. Haber,²¹ E. Hafen,²² S. R. Hahn,¹⁰ C. Hall,¹⁴ T. Handa,¹⁵ R. Handler,⁴⁴ W. Hao,³⁹ F. Happacher,¹² K. Hara,⁴¹ A. D. Hardman,³⁴ R. M. Harris,¹⁰ F. Hartmann,¹⁸ K. Hatakeyama,³⁶ J. Hauser,⁵ J. Heinrich,³¹ A. Heiss,¹⁸ M. Herndon,¹⁷ B. Hinrichsen,²³ K. D. Hoffman,³⁴ C. Holck,³¹ R. Hollebeek,³¹ L. Holloway,¹⁶ R. Hughes,²⁷ J. Huston,²⁵ J. Huth,¹⁴ H. Ikeda,⁴¹ J. Incandela,¹⁰ G. Introzzi,³² J. Iwai,⁴³ Y. Iwata,¹⁵ E. James,²⁴ H. Jensen,¹⁰ M. Jones,³¹ U. Joshi,¹⁰ H. Kambara,¹³ T. Kamon,³⁸ T. Kaneko,⁴¹ K. Karr,⁴² H. Kasha,⁴⁵ Y. Kato,²⁸ T. A. Keaffaber,³⁴ K. Kelley,²² M. Kelly,²⁴ R. D. Kennedy,¹⁰ R. Kephart,¹⁰ D. Khazins,⁹ T. Kikuchi,⁴¹ B. Kilminster,³⁵ M. Kirby,⁹ M. Kirk,⁴ B. J. Kim,¹⁹ D. H. Kim,¹⁹ H. S. Kim,¹⁶ M. J. Kim,¹⁹ S. H. Kim,⁴¹ Y. K. Kim,²¹ L. Kirsch,⁴ S. Klimentenko,¹¹ P. Koehn,²⁷ A. Köngeter,¹⁸ K. Kondo,⁴³ J. Konigsberg,¹¹ K. Kordas,²³ A. Korn,²² A. Korytov,¹¹ E. Kovacs,² J. Kroll,³¹ M. Kruse,³⁵ S. E. Kuhlmann,² K. Kurino,¹⁵ T. Kuwabara,⁴¹ A. T. Laasanen,³⁴ N. Lai,⁷ S. Lami,³⁶ S. Lammel,¹⁰ J. I. Lamoureux,⁴ M. Lancaster,²¹ G. Latino,³² T. LeCompte,² A. M. Lee IV,⁹ K. Lee,³⁹ S. Leone,³² J. D. Lewis,¹⁰ M. Lindgren,⁵ T. M. Liss,¹⁶ J. B. Liu,³⁵ Y. C. Liu,¹ N. Lockyer,³¹ J. Loken,²⁹ M. Loretto,³⁰ D. Lucchesi,³⁰ P. Lukens,¹⁰ S. Lusin,⁴⁴ L. Lyons,²⁹ J. Lys,²¹ R. Madrak,¹⁴ K. Maeshima,¹⁰ P. Maksimovic,¹⁴ L. Malferrari,³ M. Mangano,³² M. Mariotti,³⁰ G. Martignon,³⁰ A. Martin,⁴⁵ J. A. J. Matthews,²⁶ J. Mayer,²³ P. Mazzanti,³ K. S. McFarland,³⁵ P. McIntyre,³⁸ E. McKigney,³¹ M. Menguzzato,³⁰ A. Menzione,³² C. Mesropian,³⁶ T. Miao,¹⁰ R. Miller,²⁵ J. S. Miller,²⁴ H. Minato,⁴¹ S. Miscetti,¹² M. Mishina,²⁰ G. Mitselmakher,¹¹ N. Moggi,³ E. Moore,²⁶ R. Moore,²⁴ Y. Morita,²⁰ A. Mukherjee,¹⁰ T. Muller,¹⁸ A. Munar,³² P. Murat,¹⁰ S. Murgia,²⁵ M. Musy,⁴⁰ J. Nachtman,⁵ S. Nahn,⁴⁵ H. Nakada,⁴¹ T. Nakaya,⁷ I. Nakano,¹⁵ C. Nelson,¹⁰ D. Neuberger,¹⁸ C. Newman-Holmes,¹⁰ C.-Y. P. Ngan,²² P. Nicolaidi,⁴⁰ H. Niu,⁴ L. Nodulman,² A. Nomerotski,¹¹ S. H. Oh,⁹ T. Ohmoto,¹⁵ T. Ohsugi,¹⁵ R. Oishi,⁴¹ T. Okusawa,²⁸ J. Olsen,⁴⁴ W. Orejudos,²¹ C. Pagliarone,³² F. Palmonari,³² R. Paoletti,³² V. Papadimitriou,³⁹ S. P. Pappas,⁴⁵ D. Partos,⁴ J. Patrick,¹⁰ G. Pauletta,⁴⁰ M. Paulini,²¹ C. Paus,²² L. Pescara,³⁰ T. J. Phillips,⁹ G. Piacentino,³² K. T. Pitts,¹⁶ R. Plunkett,¹⁰ A. Pompos,³⁴ L. Pondrom,⁴⁴ G. Pope,³³ M. Popovic,²³ F. Prokoshin,⁸ J. Proudfoot,² F. Ptohos,¹² O. Pukhov,⁸ G. Punzi,³² K. Ragan,²³ A. Rakitine,²² D. Reher,²¹ A. Reichold,²⁹ W. Riegler,¹⁴ A. Ribon,³⁰ F. Rimondi,³ L. Ristori,³² W. J. Robertson,⁹ A. Robinson,²³ T. Rodrigo,⁶ S. Rolli,⁴² L. Rosenson,²² R. Roser,¹⁰ R. Rossin,³⁰ A. Safonov,³⁶ W. K. Sakumoto,³⁵ D. Saltzberg,⁵ A. Sansoni,¹² L. Santi,⁴⁰ H. Sato,⁴¹ P. Savard,²³ P. Schlabach,¹⁰ E. E. Schmidt,¹⁰ M. P. Schmidt,⁴⁵ M. Schmitt,¹⁴ L. Scodellaro,³⁰ A. Scott,⁵ A. Scribano,³² S. Segler,¹⁰ S. Seidel,²⁶ Y. Seiya,⁴¹ A. Semenov,⁸ F. Semeria,³ T. Shah,²² M. D. Shapiro,²¹ P. F. Shepard,³³ T. Shibayama,⁴¹ M. Shimojima,⁴¹ M. Shochet,⁷ J. Siegrist,²¹ G. Signorelli,³² A. Sill,³⁹ P. Sinervo,²³ P. Singh,¹⁶ A. J. Slaughter,⁴⁵ K. Sliwa,⁴² C. Smith,¹⁷ F. D. Snider,¹⁰ A. Solodsky,³⁶ J. Spalding,¹⁰ T. Speer,¹³ P. Sphicas,²² F. Spinella,³² M. Spiropulu,¹⁴ L. Spiegel,¹⁰ J. Steele,⁴⁴ A. Stefanini,³² J. Strologas,¹⁶ F. Strumia,¹³

D. Stuart,¹⁰ K. Sumorok,²² T. Suzuki,⁴¹ T. Takano,²⁸ R. Takashima,¹⁵ K. Takikawa,⁴¹ P. Tamburello,⁹ M. Tanaka,⁴¹ B. Tannenbaum,⁵ W. Taylor,²³ M. Tecchio,²⁴ P. K. Teng,¹ K. Terashi,⁴¹ S. Tether,²² D. Theriot,¹⁰ R. Thurman-Keup,² P. Tipton,³⁵ S. Tkaczyk,¹⁰ K. Tollefson,³⁵ A. Tollestrup,¹⁰ H. Toyoda,²⁸ W. Trischuk,²³ J. F. de Troconiz,¹⁴ J. Tseng,²² N. Turini,³² F. Ukegawa,⁴¹ T. Vaiciulis,³⁵ J. Valls,³⁷ S. Vajcic III,¹⁰ G. Velev,¹⁰ R. Vidal,¹⁰ R. Vilar,⁶ I. Volobouev,²¹ D. Vucinic,²² R. G. Wagner,² R. L. Wagner,¹⁰ J. Wahl,⁷ N. B. Wallace,³⁷ A. M. Walsh,³⁷ C. Wang,⁹ C. H. Wang,¹ M. J. Wang,¹ T. Watanabe,⁴¹ D. Waters,²⁹ T. Watts,³⁷ R. Webb,³⁸ H. Wenzel,¹⁸ W. C. Wester III,¹⁰ A. B. Wicklund,² E. Wicklund,¹⁰ H. H. Williams,³¹ P. Wilson,¹⁰ B. L. Winer,²⁷ D. Winn,²⁴ S. Wolbers,¹⁰ D. Wolinski,²⁴ J. Wolinski,²⁵ S. Wolinski,²⁴ S. Worm,²⁶ X. Wu,¹³ J. Wyss,³² A. Yagil,¹⁰ W. Yao,²¹ G. P. Yeh,¹⁰ P. Yeh,¹ J. Yoh,¹⁰ C. Yosef,²⁵ T. Yoshida,²⁸ I. Yu,¹⁹ S. Yu,³¹ Z. Yu,⁴⁵ A. Zanetti,⁴⁰ F. Zetti,²¹ and S. Zucchelli³

(CDF Collaboration)

¹*Institute of Physics, Academia Sinica, Taipei, Taiwan 11529, Republic of China*

²*Argonne National Laboratory, Argonne, Illinois 60439*

³*Istituto Nazionale di Fisica Nucleare, University of Bologna, I-40127 Bologna, Italy*

⁴*Brandeis University, Waltham, Massachusetts 02254*

⁵*University of California at Los Angeles, Los Angeles, California 90024*

⁶*Instituto de Fisica de Cantabria, CSIC-University of Cantabria, 39005 Santander, Spain*

⁷*Enrico Fermi Institute, University of Chicago, Chicago, Illinois 60637*

⁸*Joint Institute for Nuclear Research, RU-141980 Dubna, Russia*

⁹*Duke University, Durham, North Carolina 27708*

¹⁰*Fermi National Accelerator Laboratory, Batavia, Illinois 60510*

¹¹*University of Florida, Gainesville, Florida 32611*

¹²*Laboratori Nazionali di Frascati, Istituto Nazionale di Fisica Nucleare, I-00044 Frascati, Italy*

¹³*University of Geneva, CH-1211 Geneva 4, Switzerland*

¹⁴*Harvard University, Cambridge, Massachusetts 02138*

¹⁵*Hiroshima University, Higashi-Hiroshima 724, Japan*

¹⁶*University of Illinois, Urbana, Illinois 61801*

¹⁷*The Johns Hopkins University, Baltimore, Maryland 21218*

¹⁸*Institut für Experimentelle Kernphysik, Universität Karlsruhe, 76128 Karlsruhe, Germany*

¹⁹*Korean Hadron Collider Laboratory: Kyungpook National University, Taegu 702-701, Korea and SungKyunKwan University, Suwon 440-746, Korea*

²⁰*High Energy Accelerator Research Organization (KEK), Tsukuba, Ibaraki 305, Japan*

²¹*Ernest Orlando Lawrence Berkeley National Laboratory, Berkeley, California 94720*

²²*Massachusetts Institute of Technology, Cambridge, Massachusetts 02139*

²³*Institute of Particle Physics: McGill University, Montreal, Canada H3A 2T8, and University of Toronto, Toronto, Canada M5S 1A7*

²⁴*University of Michigan, Ann Arbor, Michigan 48109*

²⁵*Michigan State University, East Lansing, Michigan 48824*

²⁶*University of New Mexico, Albuquerque, New Mexico 87131*

²⁷*The Ohio State University, Columbus, Ohio 43210*

²⁸*Osaka City University, Osaka 588, Japan*

²⁹*University of Oxford, Oxford OX1 3RH, United Kingdom*

³⁰*Universita di Padova, Istituto Nazionale di Fisica Nucleare, Sezione di Padova, I-35131 Padova, Italy*

³¹*University of Pennsylvania, Philadelphia, Pennsylvania 19104*

³²*Istituto Nazionale di Fisica Nucleare, University and Scuola Normale Superiore of Pisa, I-56100 Pisa, Italy*

³³*University of Pittsburgh, Pittsburgh, Pennsylvania 15260*

³⁴*Purdue University, West Lafayette, Indiana 47907*

³⁵*University of Rochester, Rochester, New York 14627*

³⁶*Rockefeller University, New York, New York 10021*

³⁷*Rutgers University, Piscataway, New Jersey 08855*

³⁸*Texas A&M University, College Station, Texas 77843*

³⁹*Texas Tech University, Lubbock, Texas 79409*

⁴⁰*Istituto Nazionale di Fisica Nucleare, University of Trieste, Udine, Italy*

⁴¹*University of Tsukuba, Tsukuba, Ibaraki 305, Japan*

⁴²*Tufts University, Medford, Massachusetts 02155*

⁴³*Waseda University, Tokyo 169, Japan*

⁴⁴*University of Wisconsin, Madison, Wisconsin 53706*

⁴⁵*Yale University, New Haven, Connecticut 06520*

(Received 17 April 2000)

This Letter describes a direct measurement of the W boson total decay width, Γ_W , using the Collider Detector at Fermilab. The measurement uses an integrated luminosity of 90 pb^{-1} , collected during the 1994–1995 run of the Fermilab Tevatron $p\bar{p}$ collider. The width is determined by normalizing predicted signal and background distributions to 49 844 $W \rightarrow e\nu$ candidates and 21 806 $W \rightarrow \mu\nu$ candidates in the transverse-mass region $M_T < 200 \text{ GeV}$ and then fitting the predicted shape to the 438 electron events and 196 muon events in the high- M_T region, $100 < M_T < 200 \text{ GeV}$. The result is $\Gamma_W = 2.04 \pm 0.11(\text{stat}) \pm 0.09(\text{syst}) \text{ GeV}$.

PACS numbers: 13.38.Be, 12.15.Ji, 14.70.Fm

The masses and coupling strengths of the gauge bosons that mediate the known forces are fundamental parameters in the standard model (SM). The W boson width, Γ_W , is precisely predicted in terms of these masses and couplings. The leptonic partial width $\Gamma(W \rightarrow \ell\nu)$ for the lepton ℓ can be expressed as $G_F M_W^3 / 6\sqrt{2} \pi (1 + \delta_{\text{SM}})$ in terms of the well-measured muon decay constant G_F , the W boson mass M_W , and a small ($< \frac{1}{2}\%$) radiative correction δ_{SM} to the Born-level expression [1]. Dividing the partial width by the branching ratio, $B(W \rightarrow \ell\nu) = 1/\{3 + 6[1 + \alpha_s(M_W)/\pi + \mathcal{O}(\alpha_s^2)]\}$, gives the SM prediction for the full width of the W boson, $\Gamma_W = 2.093 \pm 0.002 \text{ GeV}$ [2].

The W width has been measured indirectly using the ratio $R \equiv \frac{\sigma B(p\bar{p} \rightarrow W \rightarrow \ell\nu)}{\sigma B(p\bar{p} \rightarrow Z^0 \rightarrow \ell^+\ell^-)}$ [3], with a current precision of 50 MeV [4], by assuming SM values for $\sigma(W)/\sigma(Z)$ and $\Gamma(W \rightarrow \ell\nu)$ and using the CERN Large Electron-Positron Collider (LEP) measurement of the branching ratio $B(Z \rightarrow \ell^+\ell^-)$. Direct measurements of Γ_W from line-shape analyses have been reported in $p\bar{p}$ collisions, with a precision of 320 MeV [5], and in e^+e^- collisions, where presently the most precise measurement has an uncertainty of 375 MeV [6].

The CDF collaboration previously reported [5] a direct measurement of the W width using an integrated luminosity of 20 pb^{-1} of $W \rightarrow e\nu$ data collected by CDF during the 1992–1993 run of the Fermilab Tevatron collider. This Letter extends that measurement, using a 90 pb^{-1} sample of $W \rightarrow e\nu$ and $W \rightarrow \mu\nu$ data collected by CDF during the period from January 1994 to July 1995.

This paper presents a measurement of Γ_W obtained in studies of the transverse-mass spectra of leptonic W decays. The transverse mass is defined as $M_T \equiv \sqrt{2P_T^\ell P_T^\nu [1 - \cos(\Delta\phi)]}$, where $\ell = e$ or μ , P_T^ℓ and P_T^ν are the transverse momenta [7] of the charged lepton and neutrino, and $\Delta\phi$ is the azimuthal angle between them. The transverse-mass spectrum exhibits a Jacobian edge at the W mass. Events with $M_T > M_W$ arise due to a combination of the nonzero W width and the detector resolution. A precise Γ_W measurement from the high-mass tail is possible, however, because the width component of the high- M_T line shape falls off much more slowly than the resolution component. In this analysis the W width is determined from a binned log-likelihood fit to the transverse-mass distribution in the region $100 < M_T < 200 \text{ GeV}$. The choice $M_T > 100 \text{ GeV}$ minimizes the sum in quadrature of systematic and statistical uncertainties.

The portions of the CDF detector relevant to this analysis are described briefly below. Detailed descriptions can be found elsewhere [8]. Electromagnetic and hadronic calorimeters, arranged in a projective tower geometry, cover the pseudorapidity range $|\eta| < 4.2$. In the region $|\eta| < 1.0$, a lead/scintillator electromagnetic calorimeter (CEM) measures electron energies with resolution $\sigma(E)/E = 13.5\%/\sqrt{E_T} (\text{GeV}) \oplus 1.5\%$. A cylindrical drift chamber (CTC), immersed in a 1.4 T solenoidal magnetic field, tracks charged particles in the range $|\eta| < 1.0$ with vertex-constrained momentum resolution $\sigma(p_T)/p_T = 0.09\% \times p_T (\text{GeV})$. A system of drift chambers and a steel absorber identifies muons in the region $|\eta| < 1.0$. Finally, a time-projection chamber (VTX) finds $p\bar{p}$ interaction vertices along the z axis.

Candidate $W \rightarrow e\nu$ events are required to have an electron in the central barrel region of the detector ($|\eta| < 1.0$) with CEM transverse energy $E_T^e > 25 \text{ GeV}$ and CTC transverse momentum $p_T^e > 15 \text{ GeV}$. The electron track must be isolated in the CTC, having no other track with $p_T > 1 \text{ GeV}$ within a cone in the η - ϕ space of $\sqrt{(\Delta\phi)^2 + (\Delta\eta)^2} = 0.25$ centered on the electron. The ratio of energy in the hadron (Had) and electromagnetic (CEM) calorimeter towers of the electron cluster is required to satisfy $E_{\text{Had}}/E_{\text{CEM}} < 0.055 + 0.00045E$ (GeV). The electron shower must be contained within a fiducial region of the CEM, away from calorimeter cell boundaries, and have a profile consistent with test-beam data.

Candidate $W \rightarrow \mu\nu$ events must have a CTC track with transverse momentum $p_T^\mu > 25 \text{ GeV}$. The CTC track must be well matched to a track segment in the muon chambers. The signal in the electromagnetic and hadronic calorimeters must be consistent with the passage of a minimum-ionizing particle, satisfying $E_{\text{CEM}} < 2 \text{ GeV}$ and $E_{\text{Had}} < 6 \text{ GeV}$. Trigger prescale factors, trigger efficiency, and limited azimuthal coverage reduce the $W \rightarrow \mu\nu$ acceptance by a factor ~ 2 with respect to the $W \rightarrow e\nu$ acceptance [9].

In both $W \rightarrow e\nu$ and $W \rightarrow \mu\nu$ candidate events, a transverse-momentum imbalance is required to signal the presence of the neutrino. The missing transverse energy, $\vec{\cancel{E}}_T \equiv -(\vec{P}_T^\ell + \vec{u})$, must satisfy $\cancel{E}_T > 25 \text{ GeV}$, where P_T^ℓ denotes E_T^e for electrons or p_T^μ for muons. The recoil transverse energy vector, \vec{u} , is defined as $\sum_i E_i \sin\theta_i (\cos\phi_i, \sin\phi_i)$, for calorimeter towers i with $|\eta| < 3.6$, excluding those traversed by the charged

lepton. The vector $-\vec{u}$, which includes initial state quantum chromodynamics (QCD) radiation, underlying event energy, and the products of overlapping $p\bar{p}$ interactions, is an estimator of the transverse momentum of the W . To reduce backgrounds and improve transverse-mass resolution, the recoil energy must satisfy $u < 20$ GeV. To ensure good measurements in the drift chamber and calorimeters, both electrons and muons must pass through all 84 layers of the CTC and must originate from an event vertex located within 60 cm of the detector center along the z axis. Events consistent with cosmic rays or $Z \rightarrow \ell^+\ell^-$ decays are removed. The $W \rightarrow e\nu$ sample consists of 49 844 events in the range $40 < M_T < 200$ GeV; the $W \rightarrow \mu\nu$ sample consists of 21 806 events with transverse masses in the same range.

Several background processes can mimic the W signal. The process $W \rightarrow \tau\nu \rightarrow \ell\nu\nu\nu$ has a signature similar to $W \rightarrow \ell\nu$ decays but at lower M_T . The process $Z \rightarrow ee$, where one electron is detected and the other is lost because it falls into an uninstrumented region of the detector, can produce the signature of an electron and \cancel{E}_T ; similarly, a $Z \rightarrow \mu\mu$ event can pass the $W \rightarrow \mu\nu$ selection if one muon is outside the $|\eta|$ acceptance of the CTC. Multijet backgrounds from QCD processes arise when one jet fragments into a single particle that mimics a charged lepton and another is mismeasured to produce an energy imbalance. A Monte Carlo simulation normalized to the $W \rightarrow \ell\nu$ data is used to predict the $W \rightarrow \tau\nu$ and $Z \rightarrow \ell^+\ell^-$ backgrounds. The QCD contribution is estimated from a study of nonisolated leptons in the data. $Z \rightarrow \tau\tau$ backgrounds are negligible [9]. Table I summarizes the background contributions for the $W \rightarrow e\nu$ and $W \rightarrow \mu\nu$ samples. In the $M_T > 200$ GeV region, 23 $W \rightarrow l\nu$ candidates are observed, consistent with the expectation of 20 ± 5 events.

Since the W and Z bosons share a common production mechanism and are close in mass, $Z \rightarrow \ell^+\ell^-$ decays are used extensively to model the detector's response to $W \rightarrow \ell\nu$ events. Samples of $Z \rightarrow ee$ and $Z \rightarrow \mu\mu$ candidates are selected using the same charged-lepton requirements as for $W \rightarrow \ell\nu$ candidates, with the exception that one muon from each $Z \rightarrow \mu\mu$ pair is subjected to less stringent fiducial requirements. The invariant mass must fall in the

window $70 < M^{\ell\ell} < 110$ GeV and the boson transverse momentum must satisfy $P_T^Z < 50$ GeV. There are 2012 $Z \rightarrow ee$ and 1830 $Z \rightarrow \mu\mu$ candidates, with negligible background. Using the LEP values of the Z -boson mass and width [2], the scales and resolutions of the lepton energy and momentum measurements are extracted from a fit to the Z -candidate $M^{\ell\ell}$ spectra. Additional fits to the Z data constrain the boson transverse-momentum spectra and provide an empirical model of the recoil response \vec{u} as a function of $P_T^{\ell\ell}$. Details of the recoil model can be found in Refs. [9,10]. These fits' ability to model well [9,10] the leptonic and hadronic response in $Z \rightarrow \ell\ell$ events is the basis for our confidence that the detector response is sufficiently well modeled.

The W transverse-mass spectrum is modeled using a Monte Carlo simulation that generates lowest-order diagrams of W production, $q\bar{q} \rightarrow W$, according to an energy-dependent Breit-Wigner distribution:

$$\sigma(\hat{s}) \sim \frac{\hat{s}}{(\hat{s} - M_W^2)^2 + \hat{s}^2 \Gamma_W^2 / M_W^2},$$

where $\sqrt{\hat{s}}$ is the (generally off-shell) $l\nu$ mass. The MRS-R2 [11] parton distribution functions are used. The effects of higher-order QCD diagrams for W production are included by giving the W bosons transverse momenta according to a fit to the boson momentum spectra in the $Z \rightarrow \ell^+\ell^-$ samples; a theoretical calculation [12] allows the W transverse-momentum spectrum to be derived from the Z transverse-momentum spectrum. The generator includes the effect of $W \rightarrow \ell\nu\gamma$ decays, and the effect of photon radiation on the lepton selection is accounted for in a detailed simulation. The lepton momenta are passed through a simulation of the detector response, which includes a parametric model of the \vec{u} measurement as a function of boson transverse momentum. The same kinematic and geometric cuts as in the data are applied in the simulation.

The simulation produces M_T spectra for a range of Γ_W values, from 1.0 to 3.0 GeV in 50 MeV intervals. Each spectrum is normalized, in the region $M_T < 200$ GeV, to the number of observed W candidates minus the number of expected background events, and background shapes at the rates shown in Table I are added to the predicted

TABLE I. The numbers of events in the $W \rightarrow \ell\nu$ signal samples and the estimated numbers of background events.

Channel	$W \rightarrow e\nu$		$W \rightarrow \mu\nu$	
M_T region	40–200	100–200	40–200	100–200
Events	49 844	438	21 806	196
$W \rightarrow \tau\nu$	870 ± 100	4 ± 2	440 ± 20	2 ± 2
$Z \rightarrow \ell\ell$	170 ± 85	5 ± 3	760 ± 30	5 ± 2
QCD multijets	450 ± 110	10 ± 4	175 ± 15	4 ± 3
Cosmic rays	0	0	4 ± 2	0
Backgrounds	1490 ± 170	19 ± 5	1379 ± 40	11 ± 4

spectra. A binned likelihood fit in 1 GeV bins over the region $100 < M_T < 200$ GeV returns $\Gamma_W = 2.175 \pm 0.125(\text{stat})$ GeV for the electron channel and $\Gamma_W = 1.780 \pm 0.195(\text{stat})$ GeV for the muon channel. Figure 1 shows the data with the best fits and normalized background shapes superimposed.

The systematic uncertainties in this measurement of the W width are due to effects that alter the shape of the transverse mass distribution. The most important sources of uncertainty are nonlinearity of the CEM E_T measurement (relevant only for electrons), recoil modeling, the W transverse-momentum spectrum, and backgrounds. To estimate the uncertainties due to these effects, these parameters are varied in the simulation and the simulated transverse mass spectra with the varied input parameters are fit to the nominal templates.

Linearity of the CEM energy measurement is studied by comparing CEM energies to CTC momenta over the range of energies spanned by electrons from the W and Z data samples. A fit to the form $E^{\text{meas}}/E^{\text{true}} = 1 + \epsilon(E_T^{\text{meas}} - \langle E_T \rangle)$ yields $\epsilon = (2.9 \pm 1.3) \times 10^{-4} \text{ GeV}^{-1}$; a study of $\psi \rightarrow ee$ and $Y \rightarrow ee$ events yields a consistent value of ϵ . CEM energies in the data are corrected event-by-event for this effect. Taking the uncertainty on ϵ to be $\pm 2.9 \times 10^{-4} \text{ GeV}^{-1}$ shifts Γ_W in the simulation by ∓ 60 MeV. A study of $\psi \rightarrow \mu\mu$, $Y \rightarrow \mu\mu$, and $Z \rightarrow \mu\mu$ resonances finds no evidence for nonlinearity in the momentum measurement. Varying the linearity of the momentum measurement within the bounds allowed by the

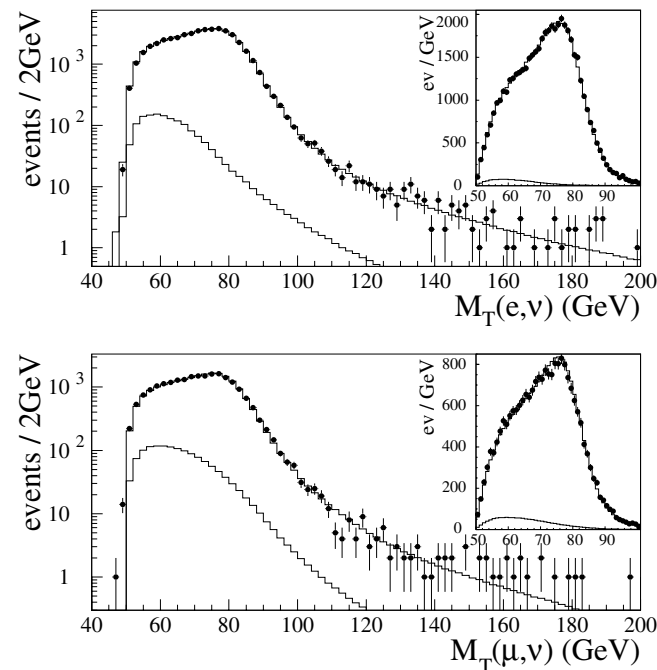


FIG. 1. Transverse mass spectra (filled circles) for $W \rightarrow e\nu$ (upper) and $W \rightarrow \mu\nu$ (lower) data, with best fits superimposed as a solid curve. The lower curve in each graph shows the sum of estimated backgrounds. Each inset shows the 50–100 GeV region on a linear scale.

data changes the muon-channel W width by only 5 MeV in the simulation.

The parameters of the recoil model are varied according to the covariance matrices obtained in the fits of \bar{u} as a function of $P_T^{\ell\ell}$ in the Z data. Because the e and μ analyses use independent fits to their respective $Z \rightarrow \ell^+\ell^-$ samples, the uncertainties are different for the two channels and are statistically independent. The effect on Γ_W is 60 MeV in the electron channel and 90 MeV in the muon channel. Similarly, the statistical uncertainty in the fits to the transverse-momentum spectra of the two Z boson samples yields a Γ_W error of 55 MeV in the electron channel and 70 MeV in the muon channel. Varying the background predictions within the errors quoted in Table I changes the electron result by 30 MeV and the muon result by 50 MeV.

Varying the muon identification cuts in the data and the muon acceptance model in the simulation yield a combined Γ_W error of 40 MeV. The muon rapidity distribution, which is modified by the acceptance of the trigger system, is fairly well modeled in the simulation [9,10], and the uncertainty quoted above represents an extreme variation in muon acceptance vs rapidity. To check the detector simulation used in the electron analysis, a sample generated using an independent simulation program is fit with the standard Γ_W templates and found to agree; the statistical precision of the check, 30 MeV, is taken as a systematic uncertainty.

Fits to the $Z \rightarrow \ell^+\ell^-$ mass spectra determine both the CEM energy and CTC momentum scales to 0.1%. Varying these scales by 0.1% in the simulation changes Γ_W by 20 and 15 MeV, respectively, in the electron and muon analyses. Varying the CEM and CTC resolutions within the uncertainties allowed by fits to the Z mass spectra varies Γ_W by 10 and 20 MeV, respectively.

Monte Carlo spectra have been generated using a variety of modern parton distribution functions, including a set whose d/u ratio was modified [13] to span the range allowed by CDF measurements of the rapidity asymmetry in $W \rightarrow \ell\nu$ decay. The rms shift in Γ_W is 15 MeV in both channels. Varying the W mass by the current world average uncertainty of 40 MeV [4,14] from the central value 80.40 GeV changes Γ_W by 10 MeV in each channel. Finally, a study comparing $W \rightarrow \ell\nu\gamma$ and $W \rightarrow \ell\nu\gamma\gamma$ in the PHOTOS [15] simulation yields a systematic uncertainty of 10 MeV. These three final sources of uncertainty are common to both analyses.

Uncertainties have been calculated separately for the fit regions $M_T > 90, 100,$ and 110 GeV. While the statistical uncertainty decreases as the cut value is lowered, the systematic uncertainty increases. The $M_T > 100$ GeV fit minimizes the total uncertainty. The results of the $M_T > 100$ and 110 GeV fits differ by 10 MeV in the electron channel and 60 MeV in the muon channel.

Table II summarizes the sources of uncertainty described above. Combining the e and μ results, with a

TABLE II. The sources of uncertainty on Γ_W for the $W \rightarrow e\nu$ and $W \rightarrow \mu\nu$ measurements. The last three uncertainties are common to the electron and muon analyses.

Source	$\Delta\Gamma (e, \text{MeV})$	$\Delta\Gamma (\mu, \text{MeV})$
Statistics	125	195
Lepton E or p_T nonlinearity	60	5
Recoil model	60	90
$W P_T$	55	70
Backgrounds	30	50
Detector modeling, lepton ID	30	40
Lepton E or p_T scale	20	15
Lepton resolution	10	20
PDFs (common)	15	15
M_W (common)	10	10
QED (common)	10	10
Total systematic	115	135
Total stat + syst	170	235

common error of 25 MeV, yields $\Gamma_W = 2.04 \pm 0.11(\text{stat}) \pm 0.09(\text{syst})$ GeV. Including the previously published CDF electron result [5] with the same common error yields $\Gamma_W = 2.05 \pm 0.10(\text{stat}) \pm 0.08(\text{syst})$ GeV. The result is in good agreement with the standard model value.

The vital contributions of the Fermilab staff and the technical staffs of the participating institutions are gratefully acknowledged. This work is supported by the U.S. Department of Energy, the National Science Foundation, the Natural Sciences and Engineering Research Council of Canada, the Istituto Nazionale di Fisica Nucleare of Italy, the Ministry of Education, Science and Culture of Japan, the National Science Council of the Republic of China, and the A.P. Sloan Foundation.

[1] J. Rosner, M. Worah, and T. Takeuchi, Phys. Rev. D **49**, 1363 (1994).

- [2] Particle Data Group, C. Caso *et al.*, Eur. Phys. J. C **3**, 1 (1998).
- [3] N. Cabibbo, in *Proceedings of the III Topical Workshop on Proton-Antiproton Collider Physics, Rome, Italy, 1983*, edited by C. Bacci and G. Salvini [CERN Report 83-04, Geneva, Switzerland, 1983 (unpublished)]; F. Halzen and M. Marsula, Phys. Rev. Lett. **51**, 857 (1983).
- [4] D0 Collaboration, B. Abbott *et al.*, Phys. Rev. D **61**, 072001 (2000); M. Lancaster, in *Proceedings of the XIX International Symposium on Lepton and Photon Interactions at High Energies, Palo Alto, CA, 1999*, edited by M. Peskin (to be published).
- [5] CDF Collaboration, F. Abe *et al.*, Phys. Rev. Lett. **74**, 341 (1995).
- [6] OPAL Collaboration, G. Abbiendi *et al.*, Phys. Lett. B **453**, 138 (1999); DELPHI Collaboration, P. Abreu *et al.*, CERN-EP/99-79 (to be published); L3 Collaboration, M. Acciarri *et al.*, Phys. Lett. B **454**, 386 (1999).
- [7] The Collider Detector at Fermilab uses a cylindrical coordinate system in which ϕ is the azimuthal angle, θ is the polar angle, and z points in the proton beam direction and is zero at the center of the detector. The pseudorapidity η is defined as $\eta \equiv \tanh^{-1}(\cos\theta)$. The transverse plane is the plane perpendicular to the z axis. The transverse energy is defined to be $E_T = E \sin\theta$.
- [8] CDF Collaboration, F. Abe *et al.*, Nucl. Instrum. Methods A **271**, 387 (1988).
- [9] CDF Collaboration, F. Abe *et al.*, hep-ex/0007044.
- [10] W.J. Ashmanskas, Ph.D. thesis, U.C. Berkeley, 1998; A. D. Hardman, Ph.D. thesis, Purdue University, 1999.
- [11] A.D. Martin, R.G. Roberts, and W.J. Stirling, Phys. Lett. B **387**, 419 (1996).
- [12] R. K. Ellis, D. A. Ross, and S. Veseli, Nucl. Phys. **B503**, 309 (1997); G. A. Ladinsky and C. P. Yuan, Phys. Rev. D **50**, 4239 (1994), and references therein.
- [13] U. K. Yang and A. Bodek, Phys. Rev. Lett. **82**, 2467 (1999).
- [14] LEP Electroweak Working Group, D. Abbaneo *et al.*, CERN-EP/99-15.
- [15] E. Barberio and Z. Was, Comput. Phys. Commun. **79**, 291 (1994).